

Production of $t\bar{t}$ pairs via $\gamma\gamma$ fusion with photon transverse momenta and proton dissociation

Marta Łuszczak,^{1,*} Laurent Forthomme,^{2,†} Wolfgang Schäfer,^{3,‡} and Antoni Szczurek^{3,§}

¹*Faculty of Mathematics and Natural Sciences,*

University of Rzeszów, ul. Pigonía 1, PL-35-310 Rzeszów, Poland

²*Helsinki Institute of Physics, P.O.Box 64 (Gustaf Hållströmin katu 2),*

FI-00014 University of Helsinki, Helsinki, Finland

³*Institute of Nuclear Physics Polish Academy of Sciences,*

ul. Radzikowskiego 152, PL-31-342 Kraków, Poland

(Dated: March 1, 2022)

Abstract

We discuss the production of $t\bar{t}$ quark-antiquark pairs in proton-proton collisions via the $\gamma\gamma$ fusion mechanism. We include topologies in which both protons stay intact or one or even both of them undergo dissociation. The calculations are performed within the k_T -factorisation approach, including transverse momenta of intermediate photons. Photon fluxes associated to inelastic (dissociative) processes are calculated based on modern parameterisations of proton structure functions. We find an integrated cross section of about 2.36 fb at $\sqrt{s} = 13$ TeV for all contributions. The cross section for the fully elastic process is the smallest. Inelastic contributions are significantly reduced when a veto on outgoing jets is imposed. We present several differential distributions in rapidity and transverse momenta of single t or \bar{t} quarks/antiquarks as well as distributions in invariant mass of both the $t\bar{t}$ and masses of dissociated systems. A few two-dimensional distributions are presented in addition.

* luszczak@ur.edu.pl

† laurent.forthomme@cern.ch

‡ wolfgang.schafer@ifj.edu.pl

§ antoni.szczurek@ifj.edu.pl

I. INTRODUCTION

Photon-induced processes in proton-proton or nucleus-nucleus interactions have become very topical recently. The large energy at the LHC, when combined with relatively large luminosity at run II, allows to start the exploration of such processes. Although in the case of proton-proton collisions the relevant cross sections are rather small, some of their salient features may allow their measurement. For instance, photon-fusion events will lead to a rapidity gap observable experimentally between the electromagnetic/electroweak vertex and forward scattered systems.

The production of electron or muon pairs are flag examples. Recently both CMS [1–3] and ATLAS [4] studied such processes. Another example is the production of W^+W^- pairs also studied by both Collaborations [5–7]. These results allow to obtain upper limits on the deviations from Standard Model couplings. On the theoretical side such processes may be calculated using the equivalent photon approximation for purely elastic and partially or fully inelastic processes [8]. The photon flux corresponding to the elastic part is then expressed in terms of electromagnetic form factors of proton (electric and magnetic, or equivalently Dirac and Pauli). Proton dissociative processes need as an input the structure functions F_2 and F_L of a proton, here especially F_2 is well known in a broad kinematic range from a large body of deep-inelastic electron-proton scattering data.

A similar method was used in the k_T -factorisation approach for dilepton production [9, 10] and recently for W^+W^- production [11]. Actually a similar approach was suggested for lepton pairs long time ago in [12] and realised in the LPAIR code [13].

Different parameterisations of the proton structure functions were used in the literature. The overall errors/uncertainties are therefore associated with insufficient knowledge of structure functions and/or poor functional form of parameterising the data. In [14, 15] it was argued that parameterisations based on proton structure functions have much smaller uncertainties, and generally lead to much smaller cross sections than in the standard DGLAP approach.

In the present approach we study a new final state, namely t and \bar{t} . Being the heaviest of fundamental Standard Model particles, the top quark is of special interest. The dominant production mechanisms investigated until recently in great detail involve the strong interactions. While the precision studies of electroweak production mechanisms are clearly the task for an e^+e^- collider [16], here we wish to investigate the $\gamma\gamma$ fusion contribution in pp collisions at the LHC.

There has not been much discussion of this final state in the literature in the context of the $\gamma\gamma$ fusion. In Ref.[17], the fully exclusive $pp \rightarrow ppt\bar{t}$ process was discussed at LHC energies, including possible anomalous $\gamma t\bar{t}$ couplings. A very comprehensive study [18] includes electroweak corrections to inclusive $t\bar{t}$ production. Being a part of these corrections, the $\gamma\gamma$ fusion subprocess is evaluated using collinear photon parton distributions. The $\gamma\gamma$ contribution to inclusive $t\bar{t}$ production is found to be negligible, when realistic photon distributions are used.

In Fig.1 we show diagrams of the four different classes of processes included in our present analysis. In the present paper we concentrate on general characteristics and study of differential distribution to select a proper observable for future experimental studies.

We wish to evaluate the cross section separately for each category presented in the figure within the Standard Model. We also aim at calculating several differential distributions of interest.

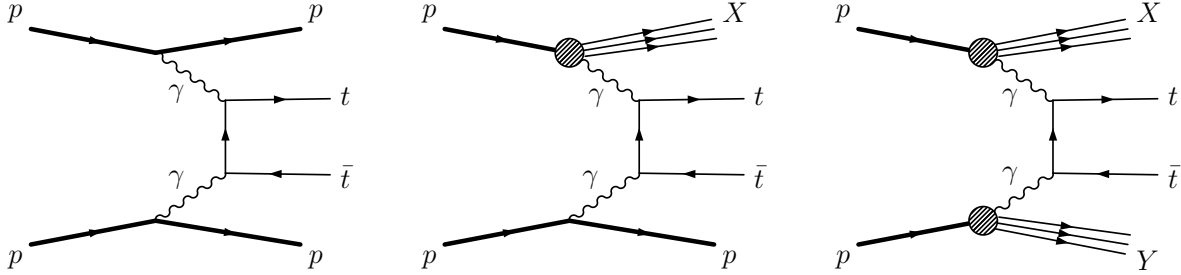


FIG. 1. Classes of processes discussed in the present paper. From left to right: elastic-elastic, inelastic-elastic (or equivalently, elastic-inelastic), and inelastic-inelastic contributions.

II. A SKETCH OF THE FORMALISM

Our calculations are based on unintegrated photon fluxes, which depend on the longitudinal momentum fraction, x and the transverse momentum (in the pp -frame) \mathbf{k} of the photon, and on the invariant mass M_X of the dissociative system in the $p \rightarrow \gamma X$ vertex:

$$\frac{d\gamma(x, \mathbf{k}, M_X)}{dM_X} = \gamma_{\text{el}}(x, \mathbf{k})\delta(M_X - m_p) + \frac{d\gamma_{\text{inel}}(x, \mathbf{k}, M_X)}{dM_X}\theta(M_X - (m_p + m_\pi)), \quad (2.1)$$

Here we put in evidence the contributions of “elastic” processes with an intact proton in the final state as well as the “inelastic” component for hadronic final states $X \neq p$.

$$\begin{aligned} \frac{d\sigma(pp \rightarrow X(\gamma^*\gamma^* \rightarrow t\bar{t})Y)}{dy_+ dy_- d^2\mathbf{p}_{T1} d^2\mathbf{p}_{T2} dM_X dM_Y} &= \int d^2\mathbf{k}_1 d^2\mathbf{k}_2 \frac{x_1 d\gamma(x_1, \mathbf{k}_1, M_X)}{dM_X} \frac{x_2 d\gamma(x_2, \mathbf{k}_2, M_Y)}{dM_Y} \times \\ &\times \frac{1}{16\pi^2(x_1 x_2 s)^2} |M(\gamma^*\gamma^* \rightarrow t\bar{t}; \mathbf{k}_1, \mathbf{k}_2)|^2 \delta^{(2)}(\mathbf{p}_{T1} + \mathbf{p}_{T2} - \mathbf{k}_1 - \mathbf{k}_2). \end{aligned} \quad (2.2)$$

In this formalism y_\pm are the rapidities and $\mathbf{p}_{T1,2}$ the transverse momenta of the t and \bar{t} quark respectively. The off-shell matrix element squared for the $\gamma^*\gamma^* \rightarrow t\bar{t}$ process is the same as the one for dilepton production found in [9], up to a factor $e_f^4 N_c$, with $e_f = +2/3$ the quark electric charge, and $N_c = 3$. In results shown below we use the top quark mass $m_t = 173 \text{ GeV}$.

These formulas are implemented in CepGen [19] for the Monte-Carlo generation of unweighted events containing the $t\bar{t}$ pair as well as remnants of mass M_X, M_Y .

Details on the relation between photon fluxes and proton structure functions may be found in [11], where we also describe several parameterisations used for F_2, F_L . Here we only mention that in the region of $Q^2 > 9 \text{ GeV}^2$, which is the most important one for the process at hand, we use a perturbative QCD NNLO calculation of [20].

III. RESULTS

In Table I we show integrated cross sections for each of the categories of $\gamma\gamma$ processes shown in Fig.1. We observe the following hierarchy as far as the integrated cross section is

| Contribution | No cuts | y_{jet} cut |
|---------------------|---------|----------------------|
| elastic-elastic | 0.292 | 0.292 |
| elastic-inelastic | 0.544 | 0.439 |
| inelastic-elastic | | |
| inelastic-inelastic | 0.983 | 0.622 |
| all contributions | 2.36 | 1.79 |

TABLE I. Cross section in fb at $\sqrt{s} = 13$ TeV for different components (left column) and the same when the extra condition on the outgoing jet $-2.5 < y_{\text{jet}} < 2.5$ is imposed.

considered:

$$\sigma_{t\bar{t}}^{\text{el-el}} < \sigma_{t\bar{t}}^{\text{in-el}} = \sigma_{t\bar{t}}^{\text{el-in}} < \sigma_{t\bar{t}}^{\text{in-in}}. \quad (3.1)$$

The summed cross section at $\sqrt{s} = 13$ TeV is 2.36 fb. This is a rather small number in comparison with other inclusive production mechanisms. A possible extraction of $\gamma\gamma$ events therefore requires, e.g. experimental cuts on rapidity gaps. So far we have ignored the gap survival factor due to remnant fragmentation and/or soft processes. However such effects may reverse the order of Eq. 3.1. This behaviour was obtained previously for production of W^+W^- pairs via $\gamma - \gamma$ fusion in [21]. In the right panel of Table I we show results when an extra condition on the rapidity of the recoiling jet, $-2.5 < y_{\text{jet}} < 2.5$, is imposed. The condition on jet rapidity gives very similar results as a condition on charged particles [21] when including explicitly remnant fragmentation.

In Fig.2 we show the rapidity distributions of t quarks or \bar{t} antiquarks (these are identical) for different categories of the final state. Quite similar distributions are obtained for the different categories of processes. There is only a small asymmetry with respect to $y = 0$ for elastic-inelastic or inelastic-elastic contributions. By construction, the sum of both the contributions is symmetric with respect to $y = 0$. The cross section is concentrated at intermediate rapidities so in principle should be measurable by the ATLAS/CMS central detectors. However, a precise estimation would require imposing cuts on the decay products of t and \bar{t} (for instance, into a b jet and a charged lepton). This goes beyond scope and aim of the present work.

In Fig.3 we show the distribution in transverse momentum of t or \bar{t} (identical). Here again the different categories give distributions of similar shape.

The same is true for the distribution in $t\bar{t}$ invariant mass (see the left panel of Fig.4). The distributions are almost identical and differ only by normalisation. For completeness in the right panel of Fig.4 we show similar results when conditions on outgoing light quark/antiquark jets are imposed. The extra condition leads to a lowering of the cross section with only very small modification of the shape in $M_{t\bar{t}}$.

In addition in Fig.5 we show distributions in outgoing proton remnant masses M_X and/or M_Y . Similar shapes are observed for single-dissociative and double-dissociative processes. Population of large M_X or M_Y masses is associated with the emissions of jets visible in central detectors (i.e. with $-2.5 < y_{\text{jet}} < 2.5$). We show the modification of the total cross section through such emissions in the right panel of the figure. The condition on jet rapidity cuts out the high mass part of distribution in M_X or M_Y . A significant correlation between maximal M_X and maximal $|y_{\text{jet}}|$ can be observed.

In Fig.6 we show distribution in photon virtuality. One may notice the photon emission through proton dissociation is much broader than that for elastic production. A large

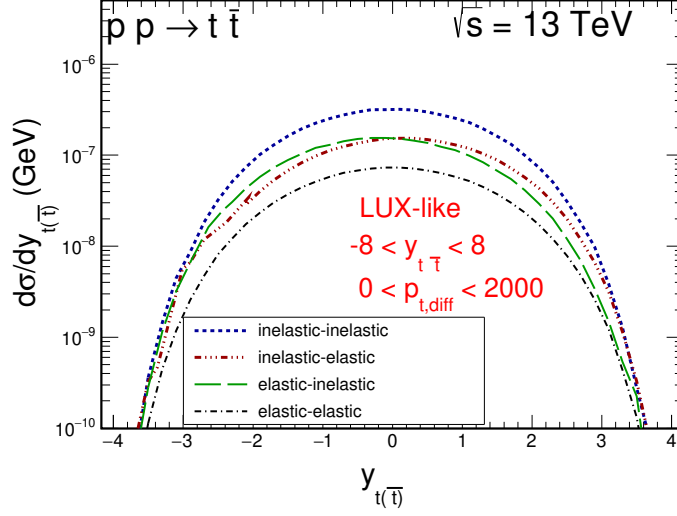


FIG. 2. Rapidity distribution for different components defined in the figure.

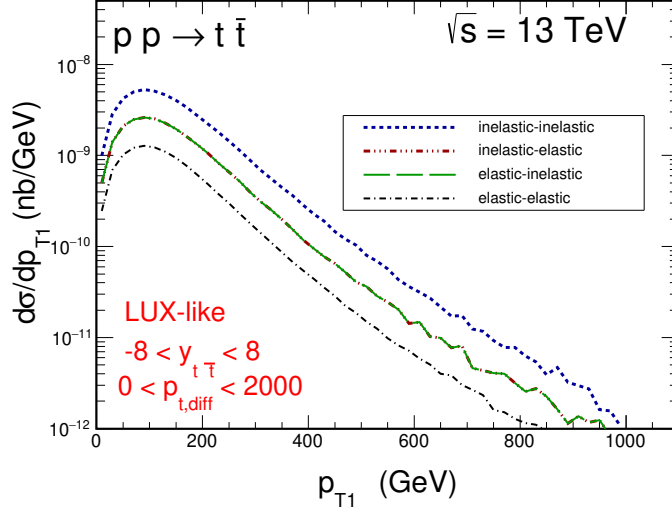


FIG. 3. Transverse momentum distribution of t or \bar{t} for different components defined in the figure.

contribution to the cross section is hence shown to arise from the region of highly virtual photons, $Q^2 > 1000 \text{ GeV}^2$.

Finally we wish to show some two-dimensional distributions in $Q_1^2 \times Q_2^2$ (Fig.7) and $M_X \times M_Y$ (Fig.8) for inelastic-inelastic case. We see regions when both virtualities are large. The apparent correlation in M_X and M_Y is only an artifact of the presentation (logarithmic scale). In fact there is no such correlation as discussed in our recent study [21]. Finally in Fig.9 we show distribution in $p_{T,\text{sum}} = |\mathbf{p}_{T1} + \mathbf{p}_{T2}|$. The distribution for the elastic-elastic component is much narrower than similar distributions for the other components. We note that for collinear photon distributions we would obtain a delta-function in $p_{T,\text{sum}}$ for all cases.

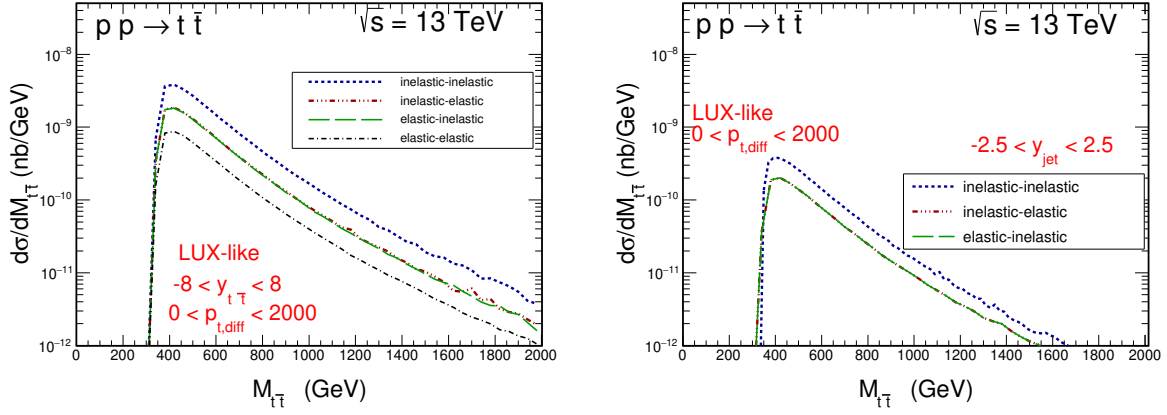


FIG. 4. $t\bar{t}$ invariant mass distribution for different components defined in the figure. The left panel is without imposing the condition on the struck quark/antiquark and the right panel includes the condition.

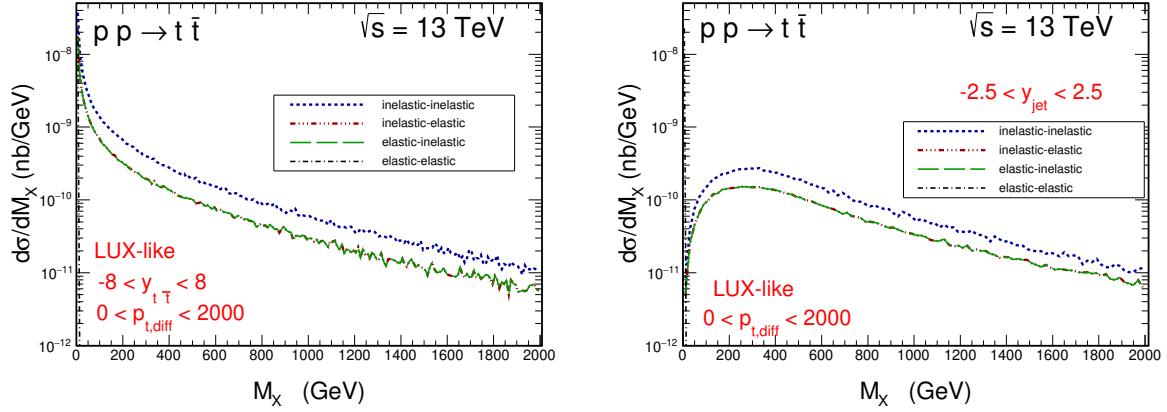


FIG. 5. Distribution in the mass of the dissociated system for different components defined in the figure. The left panel is without imposing the condition on the struck quark/antiquark and the right panel includes the condition.

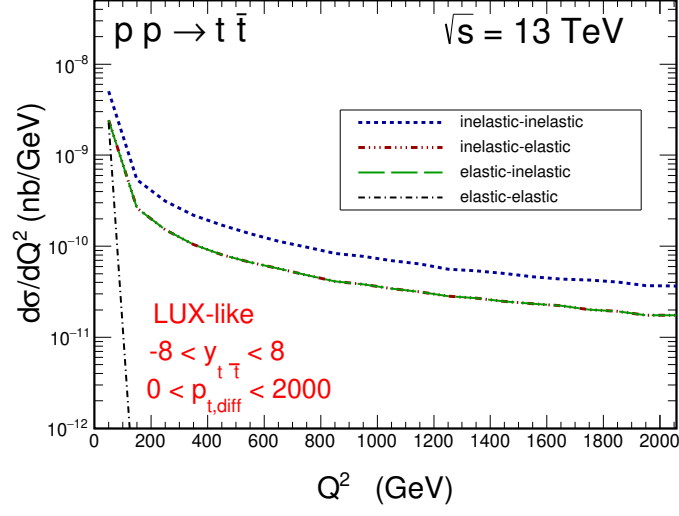


FIG. 6. Virtuality distribution for different components defined in the figure.

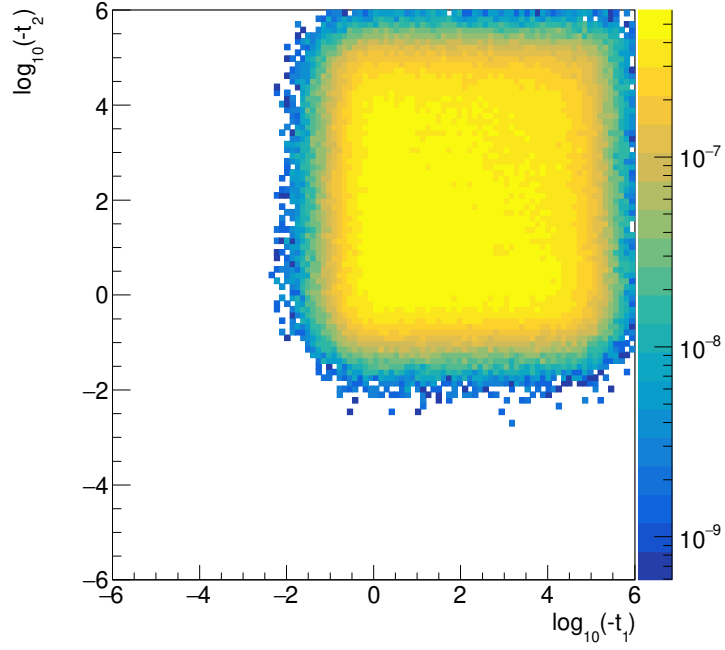


FIG. 7. Distribution in $Q_1^2 \times Q_2^2$ for the inelastic-inelastic contribution. Here $Q_i^2 = -t_i$.

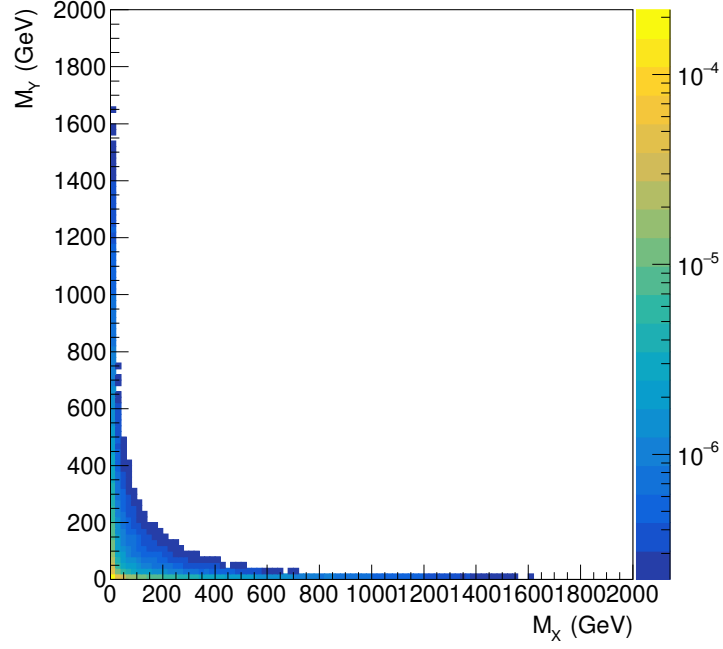


FIG. 8. Distribution in $M_X \times M_Y$ for the inelastic-inelastic contribution.

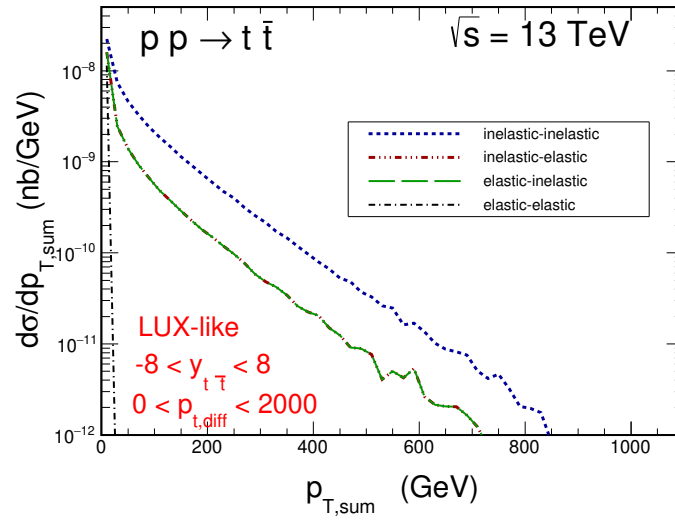


FIG. 9. Distribution in transverse momentum of the t and \bar{t} pairs for elastic - elastic, inelastic-elastic (elastic-inelastic) and inelastic-inelastic contributions for LUX-like structure function.

IV. THE GAP SURVIVAL FACTOR

Physics of the gap survival due to the jet (parton) emission was discussed in detail in Ref. [11] for the $\gamma\gamma \rightarrow W^+W^-$ production.

In this last section we wish to calculate the gap survival factor at parton level. In such a case the rapidity gap is destroyed by the outgoing parton (jet or mini-jet), which is struck by the virtual photon.

This gap survival factor may hence be defined as:

$$S_R(\eta_{\text{cut}}) = 1 - \frac{1}{\sigma} \int_{-\eta_{\text{cut}}}^{\eta_{\text{cut}}} \frac{d\sigma}{d\eta_{\text{jet}}} d\eta_{\text{jet}}, \quad (4.1)$$

where $d\sigma/d\eta_{\text{jet}}$ is the rapidity distribution of the cross section for $t\bar{t}$ production as a function of rapidity of the extra jet (de facto parton) and σ is the associated integrated cross section.

Here, in Fig.11 we show our results for $pp \rightarrow \gamma\gamma \rightarrow t\bar{t}$ processes. The gap survival factor is $S_R^{DD} < S_R^{SD}$. We have checked the factorisation $S_R^{DD} = (S_R^{SD})^2$. One may note the magnitude of such gap survival factors can reverse the ordering in (3.1) for large η_{cut} .

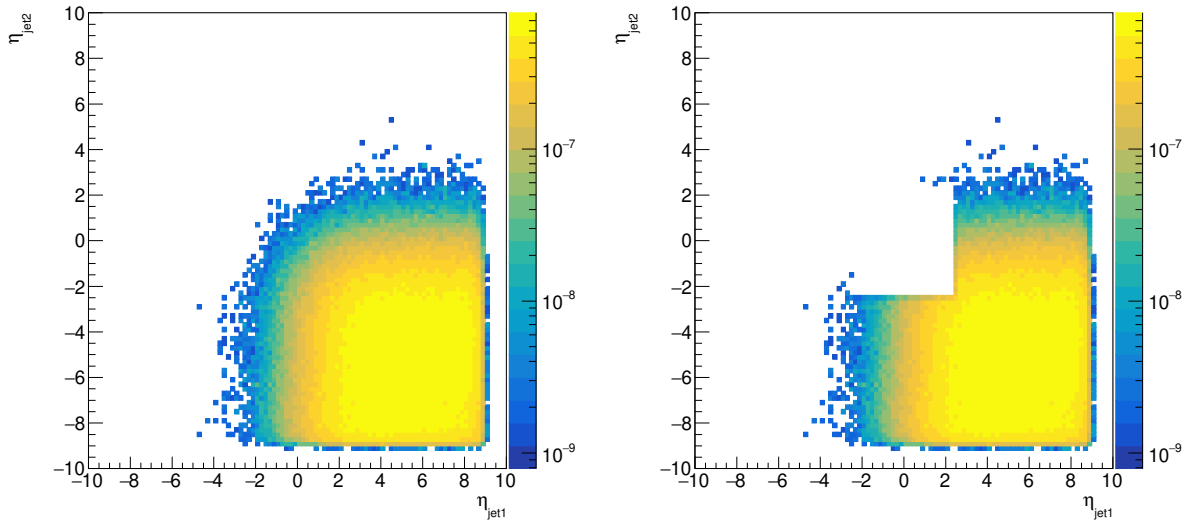


FIG. 10. Two-dimensional $(\eta_X^{\text{ch}}, \eta_Y^{\text{ch}})$ distribution without cuts (left) and with cuts (right) on η_{jet1} and η_{jet2} .

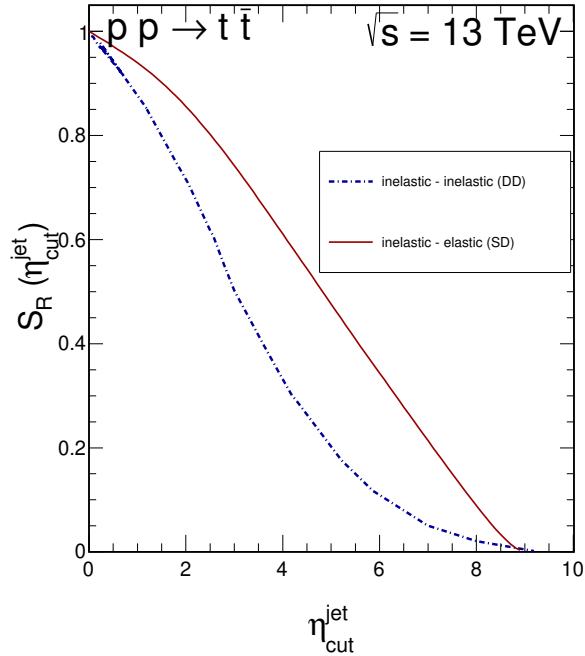


FIG. 11. Gap survival factor for single and double dissociation as a function of the size of the pseudorapidity veto applied on charged particles emitted from proton remnants.

V. CONCLUSIONS

In the present paper we have presented cross sections for production of $t\bar{t}$ pairs via $\gamma^*\gamma^*$ fusion. Such processes can be separated out by imposing rapidity gaps in the central detector. Our calculations include transverse momenta of the intermediate photons. The flux of photons produced with proton dissociation has been expressed in terms of proton structure functions. For our study we have used a hybrid parameterisation of proton structure functions, using similar input as the recent LUXqed parameterisation [15].

The cross section summed over the different categories of processes is about 2.36 fb (full phase space), i.e. rather small compared to the standard inclusive $t\bar{t}$ cross section (of the order of nb). We have shown that the ordering (3.1) holds for the whole phase space without extra experimental conditions on the top quarks decay products reconstruction efficiencies and central system gap survival factor. As discussed recently in Ref. [21] for the W^+W^- final state, the remnant fragmentation leads to a taming of the cross section when the rapidity gap requirement is imposed. Also here such a condition reverses the hierarchy observed for the case when such condition is taken into account.

One may argue that a diffractive QCD contribution leads to the same rapidity-gap topology as $\gamma\gamma$ -fusion. We have checked, that using the formalism of [22, 23], the cross section for a QCD diffractive contribution to the $t\bar{t}$ production is about 2-3 orders of magnitude smaller than the one corresponding to the photon-photon fusion and does need to be included in the final estimate.

This is very different than for “exclusive” $c\bar{c}$ [22] or $b\bar{b}$ [23] production. We have presented several differential distributions in rapidity and transverse momentum of the t or \bar{t} as well

as invariant mass of the $t\bar{t}$ system or in the mass of the dissociated proton system. We have shown also some correlation distributions, some of them two-dimensional ones.

Our results imply that for the production of such heavy objects as t quark and \bar{t} antiquark the virtuality of the photons attached to the dissociative system are very large ($Q^2 < 10^4$ GeV²). A similar effect was discussed in detail already for the W^+W^- system [11].

We have presented the best estimate of the cross section(s) and differential distributions for the inclusive case (no requirement on rapidity gap) as well as including extra condition on the jet rapidity. Applying a veto on charged particles or outgoing jet in a certain rapidity region (as done here) lowers the cross section significantly. As the gluon-gluon fusion cross section is so large, rapidity gap fluctuations in the hadronisation can be a serious background. The gap must then be chosen to minimise the unwanted contributions from gluon-gluon and quark-antiquark subprocesses not loosing too much of the signal ($\gamma\gamma \rightarrow t\bar{t}$ contribution). Evaluating such an effect will be necessary to demonstrate whether the Standard Model $\gamma\gamma \rightarrow t\bar{t}$ contribution can be “observed” at the LHC.

ACKNOWLEDGEMENTS

This study was partially supported by the Polish National Science Centre grants DEC-2014/15/B/ST2/02528 and by the Center for Innovation and Transfer of Natural Sciences and Engineering Knowledge in Rzeszów.

-
- [1] S. Chatrchyan et al. (CMS), JHEP **01**, 052 (2012), 1111.5536.
 - [2] S. Chatrchyan et al. (CMS), JHEP **11**, 080 (2012), 1209.1666.
 - [3] A. M. Sirunyan et al. (CMS, TOTEM), Submitted to: JHEP (2018), 1803.04496.
 - [4] G. Aad et al. (ATLAS), Phys. Lett. **B749**, 242 (2015), 1506.07098.
 - [5] S. Chatrchyan et al. (CMS), JHEP **07**, 116 (2013), 1305.5596.
 - [6] V. Khachatryan et al. (CMS), JHEP **08**, 119 (2016), 1604.04464.
 - [7] M. Aaboud et al. (ATLAS), Phys. Rev. **D94**, 032011 (2016), 1607.03745.
 - [8] V. M. Budnev, I. F. Ginzburg, G. V. Meledin, and V. G. Serbo, Phys. Rept. **15**, 181 (1975).
 - [9] G. G. da Silveira, L. Forthomme, K. Piotrkowski, W. Schäfer, and A. Szczurek, JHEP **02**, 159 (2015), 1409.1541.
 - [10] M. Łuszczak, W. Schäfer, and A. Szczurek, Phys. Rev. **D93**, 074018 (2016), 1510.00294.
 - [11] M. Łuszczak, W. Schäfer, and A. Szczurek, JHEP **05**, 064 (2018), 1802.03244.
 - [12] J. A. M. Vermaseren, Nucl. Phys. **B229**, 347 (1983).
 - [13] S. P. Baranov, O. Duenger, H. Shooshtari, and J. A. M. Vermaseren, in *Workshop on Physics at HERA Hamburg, Germany, October 29-30, 1991* (1991), pp. 1478–1482.
 - [14] A. Manohar, P. Nason, G. P. Salam, and G. Zanderighi, Phys. Rev. Lett. **117**, 242002 (2016), 1607.04266.
 - [15] A. V. Manohar, P. Nason, G. P. Salam, and G. Zanderighi, JHEP **12**, 046 (2017), 1708.01256.
 - [16] H. Abramowicz et al. (CLICdp) (2018), 1807.02441.
 - [17] S. Fayazbakhsh, S. T. Monfared, and M. Mohammadi Najafabadi, Phys. Rev. **D92**, 014006 (2015), 1504.06695.
 - [18] M. Czakon, D. Heymes, A. Mitov, D. Pagani, I. Tsirikos, and M. Zaro, JHEP **10**, 186 (2017), 1705.04105.

- [19] L. Forthomme (2018), 1808.06059.
- [20] A. D. Martin, W. J. Stirling, R. S. Thorne, and G. Watt, Eur. Phys. J. **C63**, 189 (2009), 0901.0002.
- [21] L. Forthomme, M. Luszczak, W. Schäfer, and A. Szczurek (2018), 1805.07124.
- [22] A. Szczurek, in *Proceedings, 14th Workshop on Elastic and Diffractive Scattering (EDS Blois Workshop) on Frontiers of QCD: From Puzzles to Discoveries: Qui Nhon, Vietnam, December 15-21, 2011* (2012), 1204.0340, URL <https://inspirehep.net/record/1097041/files/arXiv:1204.0340.pdf>.
- [23] R. Maciula, R. Pasechnik, and A. Szczurek, Phys. Rev. **D82**, 114011 (2010), 1006.3007.